

PAPER • OPEN ACCESS

Characteristic Analysis and Experimental Study of Double Layer Vibration Isolation Device

To cite this article: Bin Li *et al* 2019 *IOP Conf. Ser.: Mater. Sci. Eng.* **563** 032037

View the [article online](#) for updates and enhancements.

Characteristic Analysis and Experimental Study of Double Layer Vibration Isolation Device

Bin Li¹, Song Guo¹, Xuyao Mao¹, Biaohua Cai¹, Bo Wang¹

¹Wuhan Second Ship Design and Research Institute, Wuhan, China

libinzju@sina.com, guosongjie555@163.com, dreamforty@126.com,
cai_biaohua@sina.com, wangbo@qq.com

Abstract. Mechanical noise is an important part of underwater-radiated noise of naval vessels. With the increasing power of mechanical equipment, the running noise of equipment cannot be ignored. Noise control of ship machinery is mainly carried out in two aspects. One is to control the noise source, and the other is to control the propagation path. The application of vibration isolation device is one of the important measures to control the transmission of mechanical noise. The corresponding natural frequency and mode are obtained through modal analysis, the deformation, impact and other aspects of the vibration isolator are checked, and the stress and strain response of the system under the action of disturbing force is obtained through harmonic response analysis, and the double layer vibration isolation device is tested.

1. Introduction

Mechanical noise is an important part of underwater-radiated noise of naval vessels. With the increasing power of mechanical equipment, the running noise of equipment cannot be ignored. Noise control of ship machinery is mainly carried out in two aspects. One is to control the noise source, and the other is to control the propagation path. The application of vibration isolation device is one of the important measures to control the transmission of mechanical noise. The floating raft vibration isolation device has been widely used as an effective vibration isolation measure.

The isolation effect of the single-layer vibration isolation system in the low frequency range is very ideal, but when the excitation frequency exceeds 100Hz, the actual dynamic transfer coefficient is much higher than the theoretical value, resulting in the poor effect of medium and high frequency vibration isolation. Therefore, the application of double layer vibration isolation device can effectively improve the effect of medium and high frequency vibration isolation.

It is very important to reduce the mass of the double layer vibration isolation device under the condition of satisfying the required structural noise attenuation. The minimum mass ratio that can be selected for the double layer vibration isolation device is given as follows:

$$r = \frac{10^{L/20} + 2(f_1 / f_0)^2 - 1}{(f_1 / f_0)^4 - [10^{L/20} + 2(f_1 / f_0)^2 - 1]} \quad (1)$$

Generally, the mass ratio of the double layer vibration isolation device to the equipment is 0.5~1.1.

2. Mathematic models

In the design of the double layer vibration isolation device, the pump set is installed on the double layer vibration isolation device through the upper layer shock absorber, and the double layer vibration isolation device is installed on the equipment foundation through the lower layer vibration isolation device. The



typical structure is shown in figure 1. As the double layer vibration isolator is used for vibration isolation between the equipment and the foundation, better vibration isolation effect can be achieved in a wide range of frequencies.

Figure 2 shows the mathematic model of the double layer vibration isolation device.

Suppose the mass of the pump set is m_1 , the upper vibration isolation stiffness is k_1 , the damping of the upper vibration isolation is c_1 , the mass of the double layer vibration isolation device is m_2 , the lower vibration isolation stiffness is k_2 , and the damping of the lower vibration isolation is c_2 .

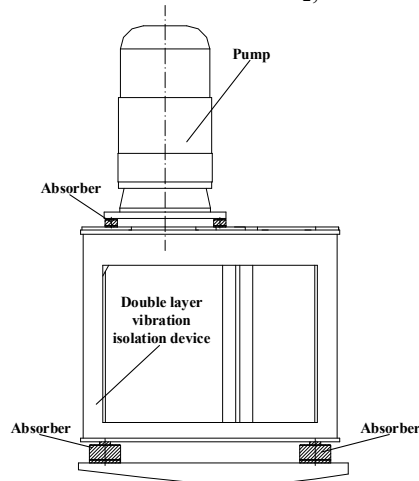


Figure 1. Diagrammatic of the double layer vibration isolation device.

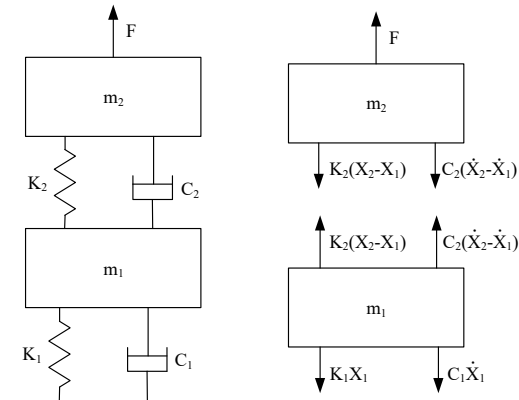


Figure 2. Mathematical model of double layer vibration isolation device.

Differential equations of motion for a mechanical model of the double layer vibration isolation system:

$$m_1 x_1 + (c_1 + c_2) \dot{x}_1 + (k_1 + k_2) x_1 - c_2 \dot{x}_2 - k_2 x_2 = 0 \tag{2}$$

$$m_2 x_2 + c_2 \dot{x}_2 + k_2 x_2 - c_2 \dot{x}_1 - k_2 x_1 = F \tag{3}$$

The frequency equation of a vibrating system:

$$\omega^4 - \left(\frac{k_2}{m_2} + \frac{k_1 + k_2}{m_1} \right) \omega^2 + \frac{k_1 + k_2}{m_1 m_2} = 0 \tag{4}$$

3. Model Analysis

The material of vibration isolation device is steel with an elastic modulus of $2.07 \times 10^7 \text{N/m}$, Poisson's ratio of 0.29, and a density of $7.9 \times 10^3 \text{kg/m}^3$.

The unit type of vibration isolation device is defined as Solid45, and vibration isolator is expressed by Combin14 unit.

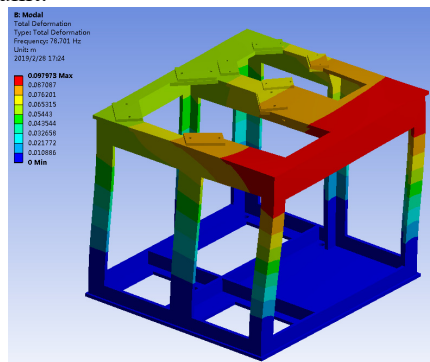


Figure 3. Deformation diagram of first order modal.

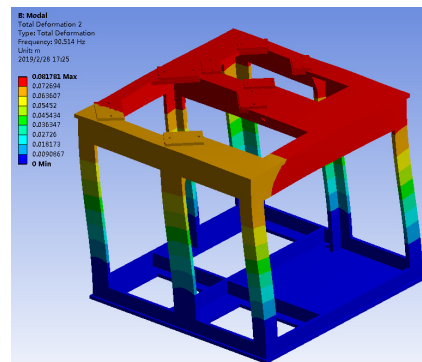


Figure 4. Deformation diagram of second order modal.

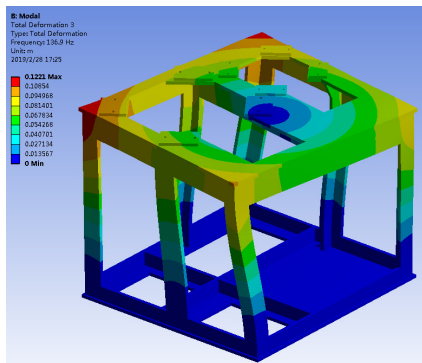


Figure 5. Deformation diagram of third order modal.

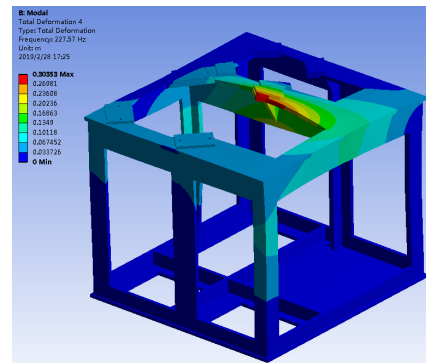


Figure 6. Deformation diagram of fourth order modal.

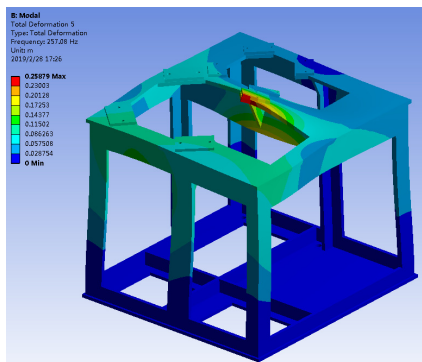


Figure 7. Deformation diagram of fifth order modal.

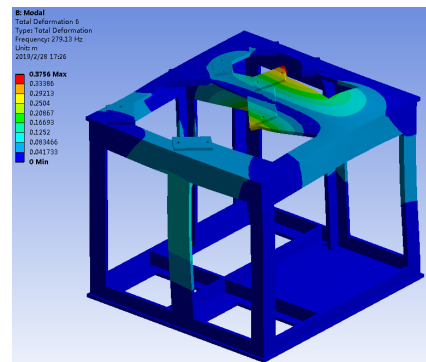


Figure 8. Deformation diagram of sixth order modal.

The deformation in the first mode is shown in figure 3, with a frequency of 78.701HZ and a maximum deformation of 0.098m; the deformation in the second mode is shown in figure 4, with a frequency of 90.151hz and a maximum deformation of 0.082m; the deformation in the third mode is shown in figure 5, with a frequency of 136.9HZ and a maximum deformation of 0.122m; the deformation in the fourth mode is shown in figure 6, with a frequency of 227.57hz and a maximum deformation of 0.304m; the deformation in the fifth mode is shown in figure 7, with a frequency of 257.08hz and a maximum deformation of 0.259m; the deformation in the sixth mode is shown in figure 8, with a frequency of 279.13hz and a maximum deformation of 0.376m. The natural frequencies of each order are shown in table 1.

Table 1. Table of natural frequencies.

| Mode | Frequency [Hz] | Mode | Frequency [Hz] |
|------|----------------|------|----------------|
| 1 | 78.701 | 4 | 227.57 |
| 2 | 90.514 | 5 | 257.08 |
| 3 | 136.9 | 6 | 279.13 |

4. Stability Analysis

Six 6JX-400 shock absorbers are set at the bottom of the double layer vibration isolation device, and four BE-220 shock absorbers are set symmetrically at the center of the pump. The static deformation of each shock absorber is shown in the table below.

Table 2. Deformation of shock absorber.

| Device name | shock absorber | Static deformation (mm) | | |
|---|----------------|-------------------------|----------------|----------------|
| | | X _j | Y _j | Z _i |
| Pump | 1#BE-220 | 0 | 0 | -2.4 |
| | 2#BE-220 | 0 | 0 | -2.5 |
| | 3#BE-220 | 0 | 0 | -2.7 |
| | 4#BE-220 | 0 | 0 | -2.6 |
| Double layer vibration isolation device | 5#6JX-400 | 0 | 0 | -4.5 |
| | 6#6JX-400 | 0 | 0 | -4.2 |
| | 7#6JX-400 | 0 | 0 | -4.9 |
| | 8#6JX-400 | 0 | 0 | -5.6 |
| | 9#6JX-400 | 0 | 0 | -5.9 |
| | 10#6JX-400 | 0 | 0 | -5.2 |

The maximum axial deformation of the shock absorber BE-220 is 2.7mm, which does not exceed the static deformation of 5mm under the rated load. The maximum Z deformation of the shock absorber 6JX-400 is 5.9mm, which does not exceed the static deformation of 14mm under the rated load. Therefore, the shock absorber layout is reasonable.

5. Frequency Response Analysis

On the basis of the above research, the response spectrum of the double layer vibration isolation device is analyzed. The given vibration acceleration in the range of 10Hz-8000Hz is shown in figure 9.

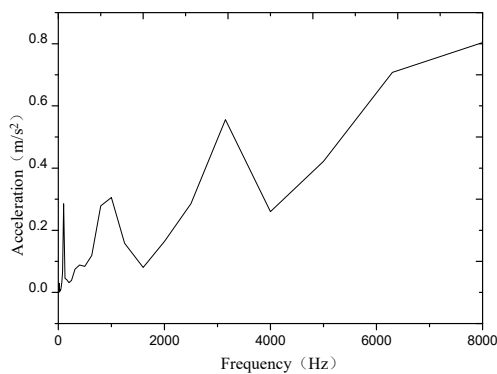


Figure 9. Input vibration acceleration curve.

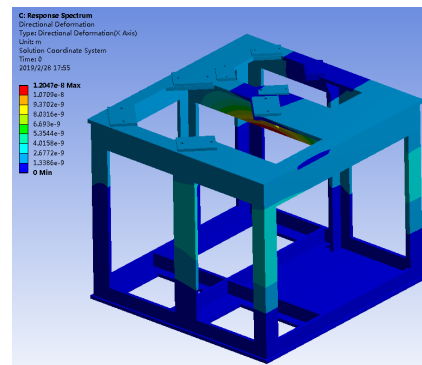


Figure 10. Directional deformation of X.

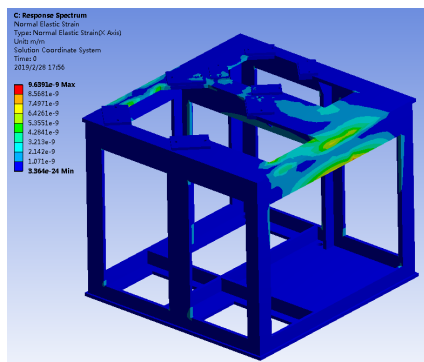


Figure 11. Normal elastic strain of device.

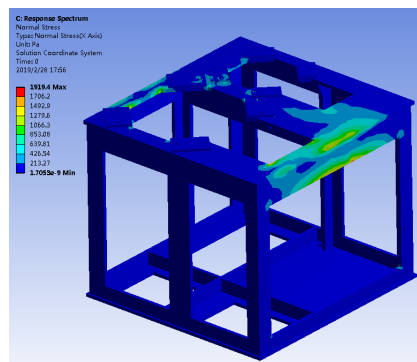


Figure 12. Normal Stress of device.

The deformation along the X-axis and the normal elastic deformation are shown in figure 10 and figure 11, and the deformation can be ignored. The stress is shown in figure 12. The maximum stress is located on the upper and outer side of the vibration isolation device, and the maximum stress is 1919.4Pa. There is no obvious stress concentration phenomenon under the response spectrum.

6. Calculation of Impact Deformation Analysis

X: Given the impact acceleration $A_1 = 72.64 \text{ m/s}^2$, impact time $t_1 = 0.0205\text{s}$.

Y: Given the impact acceleration $A_2 = 454.95\text{m/s}^2$, impact time $t_2 = 0.0082\text{s}$.

Z: Given the impact acceleration $A_3 = 302.75\text{m/s}^2$, impact time $t_3 = 0.0123\text{s}$.

The shock displacement of each shock absorber is shown in the table below.

Table 3. Table of shock displacement.

| Device name | shock absorber | +X _j | -X _j | +Y _j | -Y _j | +Z _j | -Z _j |
|---|----------------|-----------------|-----------------|-----------------|-----------------|-----------------|-----------------|
| Pump | 1#BE-220 | 0 | -2.4 | 3 | -0.0018 | 5.5 | -13 |
| | 2#BE-220 | 2.8 | 0 | 2.7 | 0 | 11 | -3.2 |
| | 3#BE-220 | 2.5 | 0 | 0.053 | -2.7 | 10 | -3.3 |
| | 4#BE-220 | 2.8 | 0 | 2.2 | -0.0071 | 5.4 | -14 |
| Double layer vibration isolation device | 9#6JX-400 | 3.1 | -6.6 | 2.7 | -0.87 | 0.032 | -3.9 |
| | 10#6JX-400 | 3.1 | -6.6 | 1.1 | -2.8 | 3.9 | 0 |
| | 11#6JX-400 | 2.2 | -4.7 | 1.1 | -2.8 | 3.9 | 0 |
| | 12#6JX-400 | 1.4 | -3.2 | 1.1 | -2.8 | 3.8 | 0 |
| | 13#6JX-400 | 1.4 | -3.2 | 2.7 | -0.87 | 0 | -4 |
| | 14#6JX-400 | 2.2 | -4.7 | 2.7 | -0.87 | 0.0081 | -3.9 |

When subjected to the above shock, the maximum deformation of the shock absorber BE-220 in the Z direction is 14mm, not exceeding the maximum allowable deformation of 36mm; the maximum Z deformation of the shock absorber 6JX-400 in the Z direction is 3.9mm, not exceeding the maximum allowable deformation of 45mm.

The above calculation results show that the preliminary design scheme of the frame structure meets the requirement of stability deformation and can ensure the structural strength under impact.

7. Experiment

The test system of the double-layer vibration isolation device is shown in figure 13, which is mainly composed of the double layer vibration isolation device, vibration sensor, amplifier, test computer and other related components.

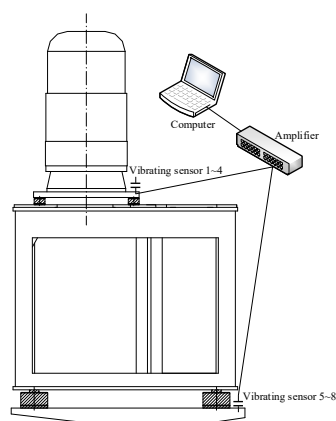


Figure 13. Experiment system of device.

Table 4. Table of the test results.

| | | | | |
|----------------------------|----------|----------|----------|----------|
| | sensor 1 | sensor 2 | sensor 3 | sensor 4 |
| Acceleration(dB) | 125 | 124 | 125 | 125 |
| | sensor 5 | sensor 6 | sensor 7 | sensor 8 |
| Acceleration(dB) | 94 | 94 | 95 | 93 |
| Vibration isolation effect | 31 | 30 | 30 | 32 |

From the perspective of vibration isolation effect, the vibration level drop distribution of the double-layer vibration isolation system at the main frequency component is mainly 20dB-35dB, which is better than the 10-20dB of the single-layer vibration isolation system, and the vibration level drop distribution of the double layer vibration isolation system at the main frequency is greater than that of the single layer vibration isolation system.

8. Conclusions

Based on the powerful dynamic analysis and processing capability of ANSYS software, the modal analysis and harmonic response analysis of the double layer vibration isolation device were carried out.

The corresponding natural frequency and mode are obtained through modal analysis, the deformation, impact and other aspects of the vibration isolator are checked, and the stress and strain response of the system under the action of disturbing force is obtained through harmonic response analysis, and the double layer vibration isolation device is tested. The test shows that the double vibration isolation effect is obvious.

References

- [1] Mizhidon A. D. Estimation of the limit possibilities of vibration isolation systems[J]. Automation and Remote Control, 2009(4), 699 - 711
- [2] Yang Tie-jun, Zhang Xin-yu, Xiao You-hong. Adaptive vibration isolation system for diesel engine[J]. Journal of Marine Science and Application, 2004(2), 30 - 35
- [3] Lee Ho-Jung, Kim Kwang-Joon. Multi-dimensional vibration power flow analysis of compressor system mounted in outdoor unit of an air conditioner[J], Journal of Sound and Vibration, 2004(272): 607 - 625
- [4] Yuichi Chida, Yoshiyuki Ishihara, Takuya Okina. Identification and frequency shaping control of a vibration isolation system[J]. Control Engineering Practice, 2008, 16(6): 711 - 723
- [5] LiXiao-jun, Chen Li-qun. Modal analysis of coupled vibration of belt drive systems, Applied Mathematics and Mechanics[J], 2008(1): 9 - 13
- [6] Mohanty P., RixenD. J. Identifying mode shapes and modal frequencies by operational modal analysis in the presence of harmonic excitation[J], Experimental Mechanics, 2005(3): 213 - 220
- [7] Fuller C, Elliot, Nelson. Active Control of Vibration, Aeademie Press, London, 1996
- [8] Dias Rodrigues J. F, Lopes H, Melo F. Q. Experimental modal analysis of a synthetic composite femur[J]. Experimental Mechanics, 2004(1): 29-32
- [9] Harris C. M, Piersol A. G. Shock and vibration handbook[M]. New York: McGraw - Hill, 2002